Promoter CAG is more efficient than hepatocyte-targeting TBG for transgene expression via rAAV8 in liver tissues

JINYU KANG[1,2], LUJIE HUANG[1], WENTAO ZHENG[1,2], JIA LUO[2], XIE ZHANG[1], YUFEI SONG[1] and AIMING LIU[2]

[1]Department of Gastroenterology, The Affiliated Lihuili Hospital, Ningbo University, Ningbo, Zhejiang 315040; [2]School of Medicine, Ningbo University, Ningbo, Zhejiang 315000, P.R. China

Received July 26, 2021; Accepted October 18, 2021

DOI: 10.3892/mmr.2021.12532

Abstract. The recombinant adeno-associated virus 8 (rAAV8) vector is a widely used tool in basic research and clinical trials. The cytomegalovirus immediate-early enhancer/chicken β-actin (CAG) promoter is a synthetic promoter used in adenoviral constructs with a wide spectrum and notable efficiency. The thyroxine binding globulin (TBG) promoter is a liver-specific promoter, which directs transgene expression in hepatocytes. However, the transduction efficiency of the rAAV vector is dependent on both the administration routes and the promoter elements. In the present study, the transduction efficiency in the liver following intraperitoneal (IP) and intravenous (IV) injections of rAAV8 with the CAG, TBG669 and TBG410 promoters was compared. Enhanced green fluorescent protein (EGFP) expression was used as the biomarker to indicate efficiency. Among the three different promoters, CAG exhibited the highest efficiency from both IV and IP injections. Following IV administration, EGFP expression, induced by the CAG promoter, was 67-fold higher compared with that in the TBG410 promoter group and 26-fold higher compared with that in the TBG669 promoter group. EGFP protein expression was higher with IV injection compared with that for IP injection for both the CAG and TBG669 promoters ($P<0.05$). With the CAG promoter, EGFP protein expression was 1.5-fold higher with the use of IV injection than with IP injection. With the TBG410 promoter, no differences were observed between the two administrations. In conclusion, these findings demonstrated that the CAG promoter was much more efficient at driving gene expression in the liver compared with that for the TBG promoters in rAAV8. In addition, IP administration produced comparable efficiency for gene delivery via the rAAV8 vector, particularly with the promoter TBG410.

Correspondence to: Dr Yufei Song, Department of Gastroenterology, The Affiliated Lihuili Hospital, Ningbo University, 57 Xingning Road, Ningbo, Zhejiang 315040, P.R. China
E-mail: songyufei2017@126.com

Dr Aiming Liu, School of Medicine, Ningbo University, 818 Fenghua Road, Ningbo, Zhejiang 315000, P.R. China
E-mail: liuaiming@nbu.edu.cn

Key words: recombinant adeno-associated virus vector, CAG promoter, TBG promoter, liver, gene therapy

Introduction

The recombinant adeno-associated virus (rAAV) vector has been widely used in a number of basic and clinical investigations (1). Compared to other viruses, the rAAV vector possesses numerous advantages for gene delivery, including a low immunogenicity, low genotoxicity, long-term gene expression, wide tissue tropism and a high transduction efficiency *in vivo* (1-3). In comparison with AAV2, the replication rate of AAV8 has been shown to be 4-10-fold faster and transgene expression is higher with AAV8 in mice (4,5). Accordingly, rAAV8 is preferred for liver gene therapy, with the induction of expression in the majority of hepatocytes and to a lesser degree in other organs, including the pancreas, spinal cord and kidney (6).

The key factors affecting the transduction efficacy of rAAV vectors include vector design, capsid selection, transgene expression cassette design and drug delivery routes (7). In transgene expression cassette design, regulatory elements and the *cis*-acting element play an important role in regulating transgene expression (8,9). The promoter is a major *cis*-acting element in the design of the expression vector, which dictates the expression, as well as cell-specificity (5,6). Promoters, with subtle changes, have a variable impact on overall transgene expression (10). The overall transgene expression can be increased by up to 90-fold with the cytomegalovirus (CMV) enhancer (11). The CMV immediate-early enhancer (CMV-IE)/chicken β-actin (CAG) promoter is a synthetic promoter (12). The CAG promoter is widely used in rAAV vectors, and exhibits a potent and long-term transcriptional activity in rodent livers (13,14). Thyroxine binding globulin (TBG) is a 54-kDa acidic glycoprotein, which is synthesized primarily in liver tissues. The TBG promoter is a liver-specific promoter, which limits transgene expression to hepatic tissues, with a low distribution in other tissues, including spleen, kidney and large intestine (15,16). Both the CAG and TBG promoters have greatly facilitated vector design in liver-targeted gene therapy (14,16). However, the direct comparison of CAG and

TBG, with routinely used administrations, has not yet been reported to date, at least to the best of our knowledge.

Delivery methods affect gene transduction efficiency and the patterns of the vectors. In the process of transduction, the intravenous (IV) injection of rAAV is the most typically used administration route (17,18). However, an IV injection requires higher technical operations with a low success rate for some investigators. Compared with other approaches, intraperitoneal (IP) administration provides several advantages, including simple technology, the minimal induction of the humoral immune response and the ability to obtain long-term transgene expression. IP injection can also transduce genes, with considerable transduction efficiency in the liver (8,19). The selection of the promoter is the key determinant of transgene expression intensity and pattern across hepatic lobules (19). However, to date, to the best of our knowledge, the transduction efficiency between the IV and IP routes has not been compared for any of the aforementioned promoters.

In the present study, the transgene expression efficiency of the CAG, TBG669 and TBG410 promoters in the rAAV8 vector in the liver via IV and IP administrations was compared. Enhanced green fluorescent protein (EGFP) protein expression was examined to indicate the working efficiency of the three promoters and two administration routes.

Materials and methods

Mouse model and viral vector administration. The animal study was approved by the Institutional Animal Care and Use Committee (approval no. IACUC 201903-138) of Ningbo University (Zhejiang, China) in March 2019. The experiment was performed in January 2020. A total of 70 male ICR mice (age, 6-8 weeks; weight, 30±2 g) were purchased from Shanghai SLAC Laboratory Animal Co., Ltd. The mice were housed at the Animal Center of Ningbo University and maintained under 12-h light/dark cycle at 24˚C, with a relative humidity of 50-70%. The mice were provided with free access to commercial rodent chow and pure water. They were cared for in accordance with the principles of the Guide for Care and Use of Experimental Animals issued by Ningbo University.

The mice were randomly divided into seven groups as follows: The control group (control; n=10), the rAAV8-treated groups by IV injection (the rAAV8-TBG410-EGFP group, the rAAV8-TBG669-EGFP group and the rAAV8-CAG-EGFP group; n=10 per group) and the rAAV8-treated groups by IP injection (the rAAV8-TBG410-EGFP group, the rAAV8-TBG669-EGFP group and the rAAV8-CAG-EGFP group; n=10 per group). The vector constructs, rAAV-TBG410-EGFP, rAAV-TBG669-EGFP and rAAV-CAG-EGFP, encoding EGFP were designed and purchased from Guangzhou PackGene Biotech Co. Ltd. The viral particles were diluted in PBS (Thermo Fisher Scientific, Inc.) at $1x10^{12}$ genome copies (GC)/ml immediately prior to injection and at a total of $1x10^{11}$ GC in 100 μl PBS was administered to the mice in the aforementioned groups via either IV or IP injection. The infusion time for each mouse was ~30 sec. The mice in the control group were left untreated.

After the administration of rAAV8, the mental state, activity, eating, hair state of the mice was observed every day. When there were significant changes in the mental state, behavior, sharp decrease in activity, sparse hair, the mice would be euthanized to avoid greater pain. In the process of the experiment, no mice showed the aforementioned symptoms and none were found dead. After 4 weeks, blood was collected from all mice by retroorbital bleeding. Then, all of the mice were euthanized using CO_2 inhalation at a low flow rate (20% of the volume of the cage per minute), with ventilation maintained for 1-2 min. The mice were confirmed dead when no breathing, no corneal reflexes and body stiffness were examined. The blood samples were centrifuged at 670 x g for 20 min at 4˚C and the serum was then stored at -80˚C until further analysis. A section of the freshly isolated liver tissue was cut and immediately fixed with 4% paraformaldehyde (PFA) solution (Shanghai Guoyao Reagent Co. Ltd.) at 4˚C for 24 h. The remaining liver tissues were kept at -80˚C for future analysis.

Western blot analysis of EGFP. Since only 13 of the 15 instrument lanes were available for western blot analysis, the livers of four mice in each group were randomly selected to compare the efficiency between IV and IP administration. When the transgene expression efficiency was compared among the three promoters in the IV and IP administration groups, three of the aforementioned four mouse livers in each group were used for western blotting. Total protein was extracted from 20 mg frozen liver tissues, stored at -80˚C, using RIPA lysis buffer, supplemented with 1% protease inhibitors (both from Beijing Solarbio Science and Technology Co., Ltd.). The samples were then adequately homogenized at 960 x g for 30 sec at room temperature using a MagNA Lyser instrument (Roche Diagnostics). Tissue debris was removed by centrifugation at 2,400 x g at 4˚C for 20 min. The protein concentration was determined using a BCA protein assay kit (Thermo Fisher Scientific, Inc.), then adjusted to 8 mg/ml. Loading buffer (5X; Beijing Solarbio Science and Technology Co., Ltd.) was then added to the sample (volume-volume, 1:4) and heated at 100˚C for 5 min. Subsequently, 5 μl/lane of the protein extract was loaded and separated using SDS-PAGE (10% separating gel; 5% spacer gel) and transferred onto PVDF membranes following electrophoresis. The membranes were then blocked with 5% skimmed milk/TBS-0.1% Tween-20 for 3.5 h at room temperature. This was followed by incubation with EGFP (1:5,000; cat. no. ab184601) or GAPDH (1:5,000; cat. no. ab181602) (both from Abcam) primary antibodies overnight at 4˚C. After washing with PB, the membranes were incubated with goat anti-mouse IgG antibody (1:5,000; cat. no. GAM001) or goat anti-rabbit IgG antibody (1:5,000; cat. no. GAR007) (both from MultiSciences) for 2 h at room temperature. Finally, the blotted membranes were exposed to ECL substrate (Advansta, Inc.), and the chemiluminescence imaging system, ChemiScope 6100 Touch, was used to capture the images. The measurement of the protein band density was performed using ImageJ software (version 1.8.0; National Institutes of Health).

Immunofluorescence. The liver sections were fixed in 4% PFA fix solution at 4˚C for 24 h. They were then sequentially dehydrated in 15 and 30% sucrose solution overnight at 4˚C, until the samples sunk. The samples were embedded in Optimal cutting temperature medium (OCT; Sakura Finetek Japan Co., Ltd.) and stored at -80˚C. The liver tissues were

cut into 10-μm-thick cryosections using a Leica cryostat (Leica Microsystems GmbH). The sections were then incubated with mouse monoclonal anti-EGFP antibody (1:100; cat. no. ab184601; Abcam) overnight at 4˚C. The sections were subsequently incubated with Alexa Fluor® 488 goat anti-mouse IgG (1:1,000; cat. 4408S; Cell Signaling Technology, Inc.) for 2 h at room temperature, followed by staining with DAPI (Sigma-Aldrich; Merck KGaA) for 10 min in the dark. The tissue sections were visualized using a Leica immunofluorescent confocal microscope (Leica Microsystems GmbH) at x200 magnification. The measurement of the fluorescence intensity was performed using Leica LAS X software (version 3.4.1; Leica Microsystems GmbH).

Biochemical analysis. To determine whether the treatment induced hepatotoxicity, the serum samples were thawed at 4˚C. The alanine aminotransferase (ALT), aspartate aminotransferase (AST), total bile acid (TBA) and total bilirubin (TBIL) activity in the serum samples was then measured using enzymatic colorimetry with the Multiskan GO plate reader (Thermo Fisher Scientific, Inc). The procedures for the analysis were performed according to the instructions provided by the kits (ALT, cat. no. H001; AST, cat. no. H002; TBA, cat. no. H101T; TBIL, cat. no. H115; all from Ningbo Medical System Biotechnology Co., Ltd.).

Histopathological analysis. The formalin-fixed liver tissues were dehydrated in a gradient ethanol series (70, 80, 90 and 100%) and washed with xylene. They were then embedded in paraffin at 56˚C and cut into 4-μm-thick sections using the Leica RM2235 Manual Rotary Microtome (Leica Microsystems GmbH) and stained with hematoxylin (cat. no. G1140) for 3 min and eosin (cat. no. G1100) (both from Beijing Solarbio Science & Technology Co., Ltd.) for 2 min at room temperature. The observation of the stained liver tissue sections was performed using an Olympus BX41 microscope (Olympus Corporation) at x100 and x400 magnifications.

Reverse transcription-quantitative PCR (RT-qPCR). The frozen liver tissues (20 mg) of five mice in each group randomly selected for RT-qPCR analysis. The liver tissues were lysed with TRIzol® (Invitrogen; Thermo Fisher Scientific, Inc.) and homogenized at 960 x g for 30 sec at room temperature using a MagNA Lyser instrument (Roche Diagnostics). Pure chloroform was then added for 5 min to extract total RNA at room temperature. This was followed by centrifugation at 3, 200 x g for 15 min at 4˚C and precipitation with 75% ethanol. The RNA concentration was quantified using the Multiskan GO plate reader (Thermo Fisher Scientific, Inc) and its purity was determined using the OD260/OD280 calculation. Total RNA was reverse transcribed into cDNA using RT (20 μl; cat. no. CW2569M; CoWin Biosciences Co., Ltd.) as previously described (20). The RT temperature protocol was as follows: 25˚C for 5 min, 42˚C for 1 h, inactivation at 70˚C for 5 min and chilling at 4˚C for holding. The primer sequences are presented in Table SI. qPCR was performed in 96-well plates using a 5-μl system containing 1 μl total cDNA, 2.2 μl UltraSYBR Mixture (cat. no. CW0957H; CoWin Biosciences Co., Ltd.), 0.1 μl forward and reverse primer, and 1.6 μl RNase-free water using the LightCycler 480 II system (Roche Diagnostics). The following thermocycling conditions were used: Initial denaturation at 95˚C for 10 sec, 55˚C for 10 sec and 72˚C for 15 sec. The $2^{-\Delta\Delta Cq}$ formula was used to quantify the expression levels of target genes (21). The measured mRNA abundance was normalized to *18S rRNA*. The expression levels in the control group were set to 1, and the data of the other six groups were normalized and expressed as relative expression.

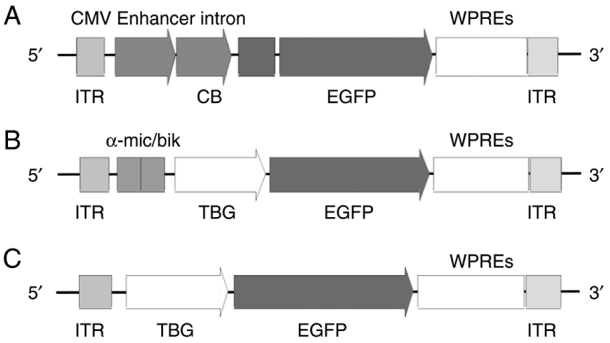

Figure 1. Schematic representation of the three rAAV8 constructs. Schematic structure of (A) rAAV8-CAG-EGFP, (B) rAAV8-TBG669-EGFP and (C) rAAV8-TBG410-EGFP vector. rAAV, recombinant adeno-associated virus; CMV, cytomegalovirus; CB, chicken β-actin promoter; α-mic/bik, an enhancer element; ITR, inverted terminal repeats; EGFP, enhanced green fluorescent protein; WPRE, woodchuck post-transcriptional regulatory element; TBG, thyroxine-binding globulin promoter; CAG, cytomegalovirus immediate-early enhancer/chicken β-actin.

Statistical analysis. The data are presented as the mean ± SEM. Data analysis was performed using SPSS version 23 software (IBM Corp.) and column charts were generated using GraphPad Prism software (version 8.0; GraphPad Software, Inc.). Statistically significant differences were determined using one-way ANOVA followed by Tukey's post hoc test for multiple comparisons. When data were not normally distributed, the Kruskal-Wallis test was used for the determination of differences among groups and Bonferroni's post hoc test was used for multiple comparisons. $P<0.05$ was considered to indicate a statistically significant difference.

Results

Schematic presentation of the three rAAV8 vectors. The schematic presentation of the three different rAAV8 vectors used in the present study was presented in Fig. 1. rAAV8 vector constructs encoding EGFP were transduced, driven by the CAG, TBG669 and TBG410 promoters. An equal concentration of $1x10^{11}$ GC in 100 μl PBS was delivered to the ICR mice via either IP or IV injection. At 4 weeks after the injection, the mice were euthanized, and blood and liver tissues were collected for analysis.

EGFP expression driven by the CAG promoter is the highest. Western blot analysis was performed to determine the protein expression level of EGFP among the three promoters, under the same administration routes. As shown in Fig. 2, the protein expression level of EGFP was the highest in the rAAV8-CAG-EGFP group, by both administration routes. With IV administration, significant differences were observed between the control, TBG410, TBG669 and CAG

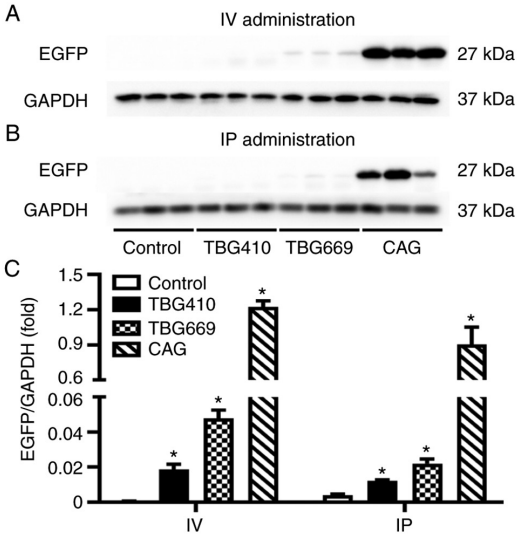

Figure 2. Comparison of the rAAV8 transduction efficiency with three different promoters. The EGFP protein expression level in the liver was analyzed using western blot in the control, TBG410, TBG669 and CAG promoter groups administered via (A) IV and (B) IP. (C) Semi-quantification of the western blots for the control, rAAV8-CAG-EGFP, rAAV8-TBG410-EGFP and rAAV8-TBG669-EGFP groups. The control group used for IV and IP groups was the same without any treatment. The livers of three mice in each group were used for western blot analysis and each lane represented an individual mouse. The data are presented as the mean ± SEM. n=3. *P<0.05 vs. control. IV, intravenous; IP, intraperitoneal; CAG, cytomegalovirus immediate-early enhancer/chicken β-actin; EGFP, enhanced green fluorescent protein; rAAV, recombinant adeno-associated virus; TBG, thyroxine-binding globulin promoter.

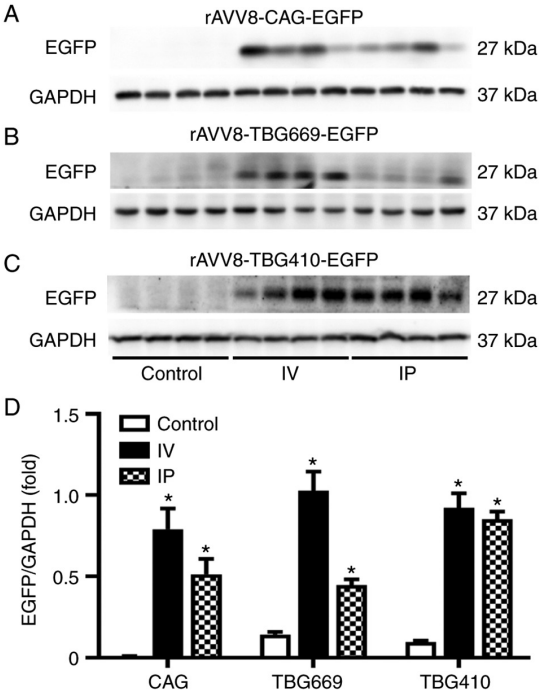

Figure 3. Comparison of the rAAV8 transduction efficiency between IV injection and IP injection. (A) The EGFP protein expression level in the liver was analyzed using western blot analysis in the (A) rAAV8-CAG-EGFP, (B) rAAV8-TBG669-EGFP and (C) rAAV8-TBG410-EGFP groups after IV and IP injection. (D) Semi-quantification of the western blots for the control, rAAV8-CAG-EGFP, rAAV8-TBG410-EGFP and rAAV8-TBG669-EGFP groups. The group without any treatment was used as the control group for both IV and IP administrations. The livers of four mice in each group were used for western blot analysis and each lane represented an individual mouse. The data are presented as the mean ± SEM. n=4. *P<0.05 vs. control. IV, intravenous; IP, intraperitoneal; CAG, cytomegalovirus immediate-early enhancer/chicken β-actin; EGFP, enhanced green fluorescent protein; rAAV, recombinant adeno-associated virus; TBG, thyroxine-binding globulin promoter.

groups., EGFP protein expression level induced by the CAG promoter was 67-fold higher compared with that in the rAAV8-TBG410-EGFP group and 26-fold higher compared with that in the TBG669 group. Gene transduction induced by the TBG669 promoter was almost 3-fold higher than that induced by the TBG410 promoter (Fig. 2A). Similarly, with the IP administration, the EGFP expression level in the rAAV8-CAG-EGFP group was 75-fold higher compared with that in the TBG410 group, and 41-fold higher compared with that in the TBG669 group (Fig. 2B).

IV delivery is more efficient than IP delivery in the liver. The comparison of the two administration routes also revealed notable results. Driven by the CAG promoter, the abundance of EGFP was significantly increased; the ratio of EGFP/GAPDH in the control, IV and IP groups was 0.008, 0.791 and 0.513, respectively. The protein expression level of EGFP with the IV and IP injections was 99- and 64-fold higher compared with that in the control group, respectively (Fig. 3A). In the rAAV8-TBG669-EGFP group, the ratio of EGFP/GAPDH in the control, IV and IP groups was 0.142, 1.027 and 0.446, respectively. EGFP protein expression with the IV injection was 2-fold higher compared with that in the IP injection group (Fig. 3B). Generally, EGFP protein expression via the IV route was superior than that via the IP route, with all vectors. However, driven by the CAG promoter and compared with that in the other two promoters, the ratio of EGFP/GAPDH in the control, IV and IP groups was 0.097, 0.922 and 0.853, respectively. EGFP protein expression was similar between both delivery routes (Fig. 3C).

Immunofluorescence analysis of EGFP expression in the liver. The EGFP expression patterns were assessed using a fluorescence microscope to confirm the quantification of the densitometric analysis. The representative fluorescent micrographs of the CAG promoter with IV and IP administrations are presented in Fig. 4. In the rAAV8-CAG-EGFP group, a robust transduction was observed, and gene expression mainly transduced in the nucleus around the central veins. In addition, the EGFP intensity was close to 4-fold higher via the IV injection compared with that via IP injection (Fig. S1). With respect to the TBG669 and TBG410 promoters, their transgene efficiency was in accordance with that observed with western blot analysis described above (data not shown).

All rAAV8 vectors exhibit sufficient safety profiles. A total of three different analyses were performed to evaluate the safety of the three rAAV8 vectors used in the present study. Biochemically, the serum ALT, AST, TBA and TBIL levels exhibited no significant changes among the three rAAV8 vectors (Fig. 5). In addition, no liver injury or inflammation was observed in any of the groups (Fig. 6). The high magnification images revealed no evidence of cellular damage and an inflammatory response (Fig. S2), supporting the aforementioned and biochemical data. Compared with that in the control

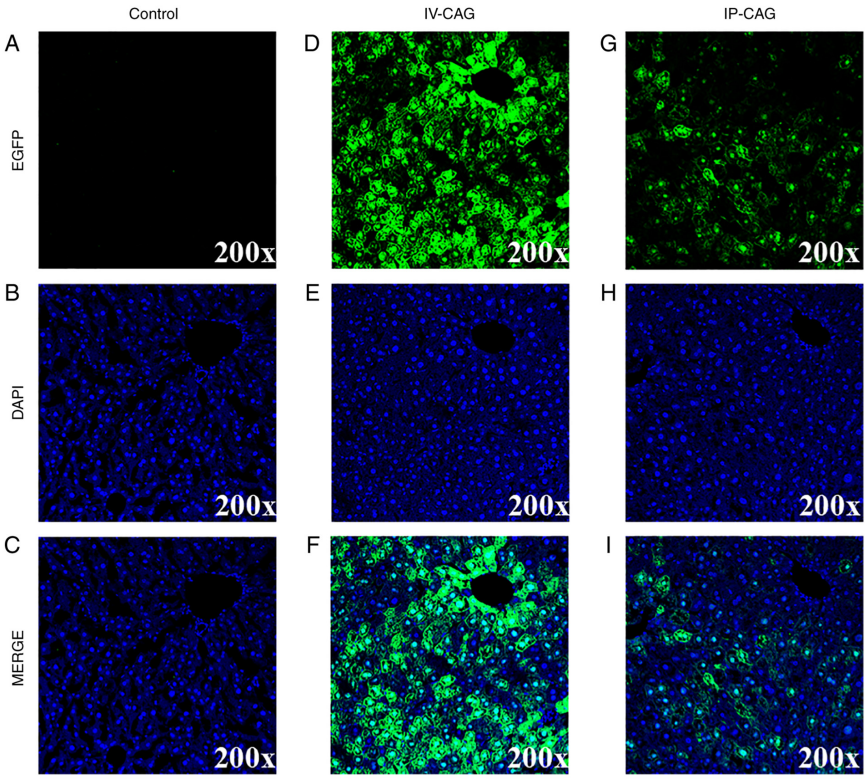

Figure 4. Immunofluorescence staining in the liver after gene transduction with rAAV8 expressing EGFP driven by the three different promoters. Representative immunofluorescence staining of the liver tissues images at magnification x200 in the (A-C) Control, (D-F) rAAV8-CAG-EGFP and (G-I) rAAV8-CAG-EGFP groups after IV and IP injection, respectively. The liver tissues sections were stained with antibodies against EGFP (green). The nucleus was counterstained with DAPI (blue). The overlay of both stains is shown in the last row. EGFP, enhanced green fluorescent protein; DAPI, 4,6-diamidino-2-phenylindole. IV, intravenous; IP, intraperitoneal; CAG, cytomegalovirus immediate-early enhancer/chicken β-actin promoter; rAAV, recombinant adeno-associated virus.

group, the mRNA expression levels of chemokine ligand 2, *Tnf-α,* suppressor of cytokine signaling 3 and fibrinogen α chain in the other six groups exhibited no significant differences (Fig. 7). These results suggested that the three rAAV8 vectors did not cause inflammatory responses.

Discussion

rAAV is the most promising gene therapy vehicle, as the vector itself does not affect gene expression. When a functional protein is inserted into the rAAV vector, it can increase or decrease gene expression and affect the organism or the disease model. How much it will affect the organism or the disease model depends on the action of the functional protein itself. The promoter used is crucial for the gene transduction efficiency of the rAAV vectors (10). The CAG promoter is a composite promoter, connecting the CMV-IE enhancer sequence to the chicken β-actin promoter (22). It has been used for >30 years and a number of gene therapies have made use of this promoter to achieve a high vector expression (22,23). In previous studies using AAV-mediated RPE65 transfer to retinal pigment epithelium as gene therapy for Leber congenital amaurosis, AAV vectors with the CAG promoter achieved stable RPE expression, and restoration of rod and cone photoreceptor function for several years (24,25).

The TBG promoter is a liver-specific promoter, which confers transgene persistently and specific expression to the liver for up to several months following integration (26). The TBG promoter limits transgene expression to hepatic tissue with a low distribution in other tissues. Therefore, this promoter minimizes undesired toxicity or host immune responses derived from the overexpression of the transgene outside the liver (15). Quantitively, the efficiency of the TBG promoter has been reported to be slightly lower than that of the ubiquitous CMV promoter in driving foreign gene expression (16). However, in the present study, with IV administration, a significant induction of EGFP protein expression occurred in the rAAV8-CAG-EGFP group. EGFP expression, driven by the CAG promoter, was much higher than those driven by the TBG410 and the TBG669 promoter (67- and 26-fold respectively, Fig. 2A). Similarly, with IP administration, EGFP expression was as high as those of IV administration (Fig. 2B). With respect to the TBG410 and TBG669 promoters, EGFP expression was close to 3-fold higher by the TBG669 promoter than by the TBG410 promoter in the IV group, and 1.8-fold in the IP group (Fig. 3). This occurred as an α-mic enhancer was added to the TBG669 promoter.

A number of factors affect rAAV vector transduction efficiency, such as AAV serotype tropism (1), transgene expression cassette design (9,27,28), the pattern of administration (18) and the time of injection (29,30). In IP administration, rAAVrh.10 showed robust transduction in skeletal muscle, rAAV8 showed efficient transduction in the pancreas, and rAAV9 and rAAV7 showed the strongest transduction in the liver (1). The transgene expression cassette contains an enhancer, promoter, and various pre- and/or post-regulatory elements. All of them function to achieve a higher expression of the rAAV (27). Enhancers were recognized as *cis*-regulatory DNA elements,

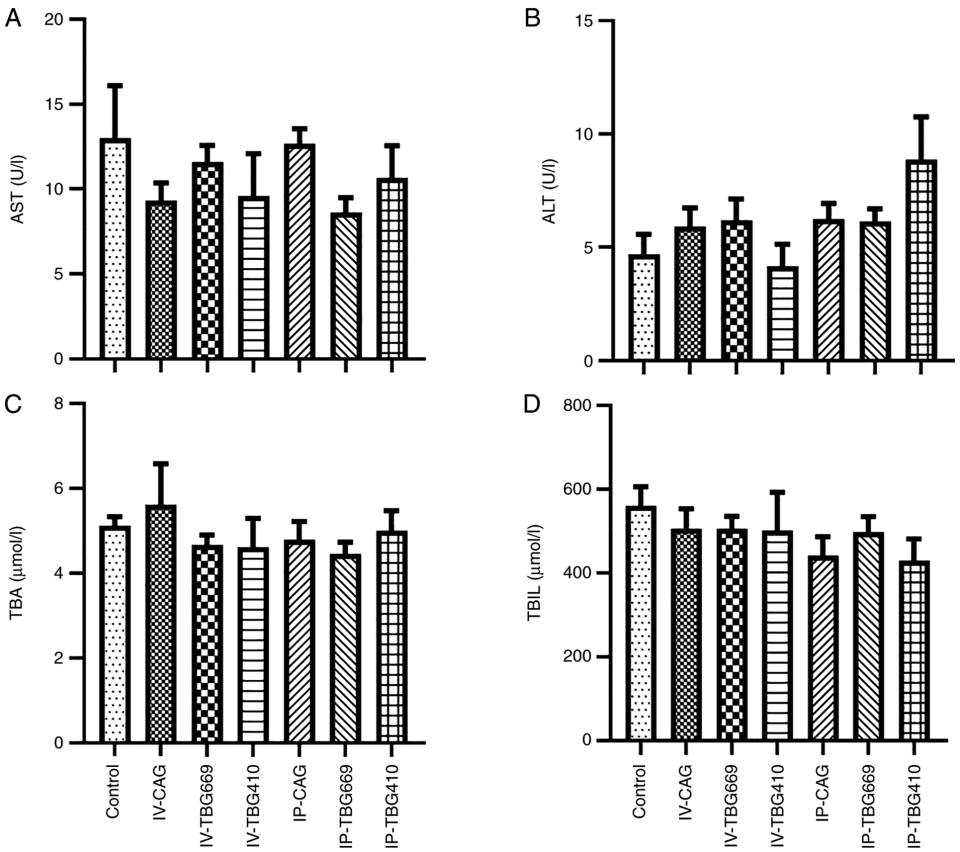

Figure 5. Hepatic injury biomarkers in mice treated with rAAV8 vectors did not increase. (A) AST, (B) ALT, (C) TBA and (D) TBIL levels in seven groups, four weeks after rAAV8 administration. n=5. ALT, alanine aminotransferase; AST, aspartate aminotransferase; TBA, total bile acid; TBIL, total bilirubin; rAAV, recombinant adeno-associated virus; IV, intravenous; IP, intraperitoneal.

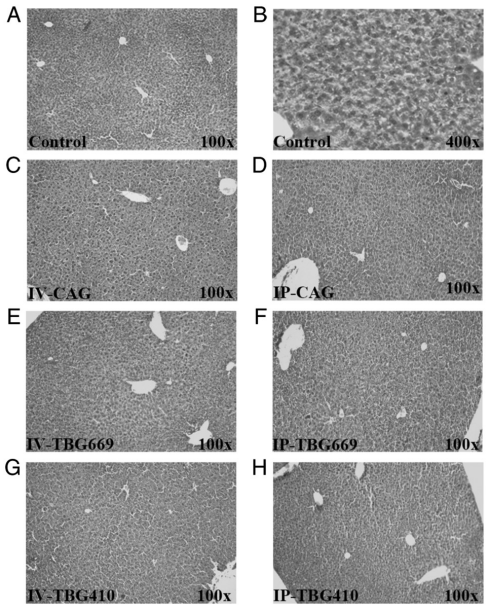

Figure 6. rAAV8 vector shows safety in histopathology. Representative H&E staining images at (A) x100 and (B) x400 magnification in the control group. Representative H&E staining of liver tissues at x100 magnification by (C) IV and (D) IP routes in the rAAV8-CAG-EGFP group. Representative H&E staining of liver tissues at x100 magnification by (E) IV and (F) IP routes in the rAAV8-TBG669-EGFP group. Representative H&E staining of liver tissues at x100 magnification by (G) IV and (H) IP routes in the rAAV8-TBG410-EGFP group. H&E, hematoxylin and eosin; rAAV, recombinant adeno-associated virus; IV, intravenous; IP, intraperitoneal; CAG, cytomegalovirus immediate-early enhancer/chicken β-actin; EGFP, enhanced green fluorescent protein; TBG, thyroxine-binding globulin promoter.

which can increase the expression of target genes in cooperation with promoters (9). Within an enhancer sequence, there are multiple transcription factor binding sites that are required for the regulation of enhancer activity (28). According to the administration routes, the transduction efficiency in cirrhotic livers is lower compared with that in healthy livers, when the vector is administered via IP injection (18). The injection/infusion rate appears to be inversely proportionate to the gene transduction efficiency. A longer infusion time has been found to produce a higher transduction efficiency than the peak administration concentration. It was considered to be associated with the time of exposure to the rAAV vector (29).

The pattern of virus injection is also one of the factors affecting efficiency. In the present study, transgene expression with IV injection was more efficient than that with IP injection in the liver. However, the efficiency of TBG410 was similar between both delivery routes. When one wants to choose the administration of a virus, IP injection can also be considered, especially when IV injection was considered difficult for numerous investigators.

In a previous study investigating AAV9-CMV-GFP and AAV9-CBA-GFP vectors, it was found that the gene transfection efficiency increased in a time-dependent manner (30). The transduction efficiency of AAV9-CBA-GFP in the liver reached 60% in the second week and maintained a high level of expression of >80% after the fourth week. The expression level of GFP reached peak levels at 5 weeks following virus injection. Certainly, it is interesting to investigate the dynamic

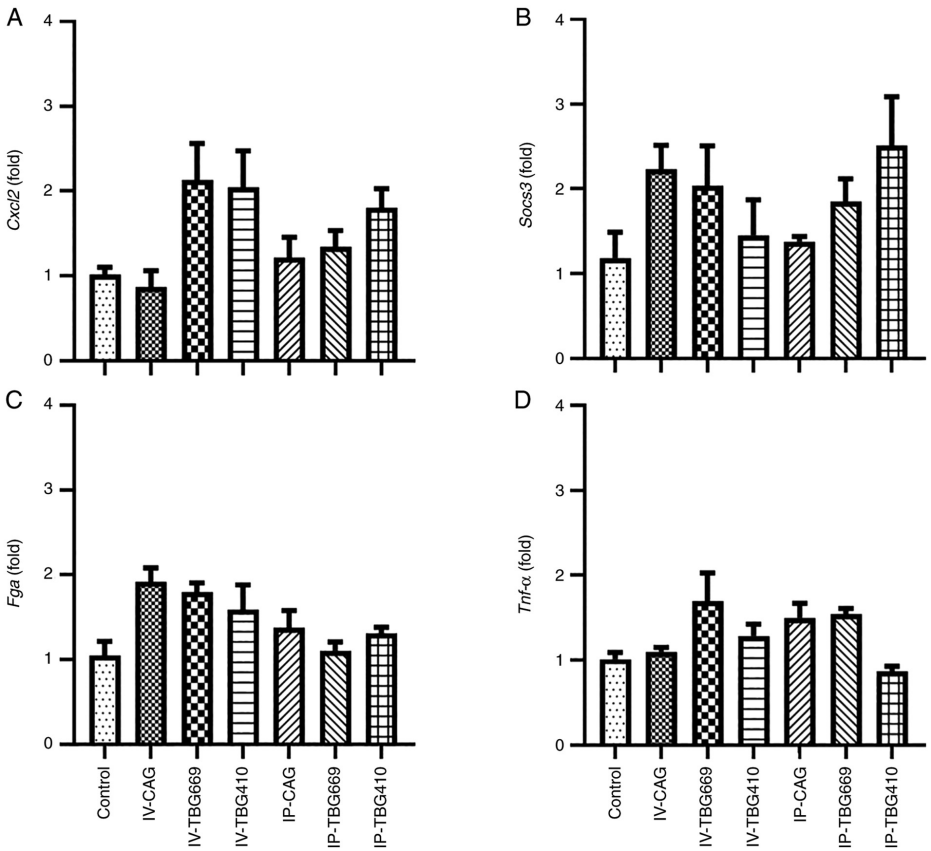

Figure 7. mRNA expression levels of genes involved in inflammatory response. (A) *Cxcl2*, (B) *Socs3*, (C) *Fga* and (D) *Tnf-α* mRNA expression in the seven groups. The mRNA expression levels were analyzed using reverse transcription-quantitative PCR and normalized to 18S ribosomal RNA. mRNA expression levels in the vehicle-treated control mice were set as 1 and the results were expressed as the mean ± SEM. n=5. Cxcl2, chemokine ligand 2; Tnf-α, tumor necrosis factor-α; Socs3, suppressor of cytokine signaling 3; Fga, fibrinogen α chain.

changes of expression efficiency of rAAV after administration, and to compare them between IV injection and IP injection. In the present study, the gene transduction efficiency was compared between three different promoters in two types of administration routes. The mice are usually sacrificed at 3-4 weeks following the injection to detect gene expression (31-33). Therefore, in the present study, the mice were sacrificed at 4 weeks. The choice of sacrificing the mice at 4 or 5 weeks may not have had a notable impact on the results.

According to the results obtained, compared with that in the CAG promoter, the hepatocyte-targeting TBG promoters led to a lower protein expression level of EGFP. However, the TBG promoter is still widely used as a hepatocyte-targeting promoter (26,34,35). When compared with that in the control, the TBG promoter could still be effectively transduced in the liver. The efficiency of the TBG669 promoter with the IV injection was 2-fold higher compared with that for IP injection (Fig. 3B). The efficiency of the TBG410 promoter was similar between both delivery routes (Fig. 3C). Therefore, if gene expression in extrahepatic tissue affects the disease model, the TBG promoter remains an adequate choice. However, the molecular mechanism is still unclear as to why the transfection efficiency of the CAG promoter was higher than that of hepatocyte-targeting TBG promoter in the liver.

rAAV vectors as gene therapy vectors are widely used in clinical practice and have exhibited efficacy in a growing number of clinical trials, with the majority of data suggesting that they are non-pathogenic (3,36). However, some experimental studies have reported evidence of the potential genotoxicity of rAAV vectors (31,36). rAAV may result in cancer development, with hepatocellular carcinoma (HCC) being the most likely malignancy (37,38). The AAV vector dose, enhancer/promoter selection and the timing of gene delivery were all critical factors for determining HCC incidence after AAV gene delivery (36). Compared with that in the healthy adult liver, rAAV gene therapy induces HCC at a high frequency in mice with chronic liver disease (35). In addition, the transduction of hepatic tissue by AAV vectors has been reported to be inefficient in mice with chronic liver disease (39). Extremely high doses ($2x10^{14}$ GC/kg) of AAV have been shown to result in acute toxicity in non-human primates (40). However, this high dose of AAV9 has been used in patients with spinal muscular atrophy type 1 in a clinical trial, without any severe treatment-related adverse events (41). There may be a threshold for the toxicity of rAAV; however, the doses currently used in the majority of clinical trials are much lower than this threshold (42). Furthermore, the enhancer-promoter may be involved in tumorigenesis in the liver (43). When compared to other promoters, AAV vectors with a TBG promoter significantly increase risk of tumorigenesis (36,44).

In conclusion, the present study demonstrated that the ubiquitous CAG promoter induced a higher EGFP expression level than hepatocyte-targeting TBG promoters via both IV and IP

administration. Although less effective than IV administration, the IP injection exhibited a satisfactory efficiency with a high success rate of procedure for the three promoters. In particular, for the TBG410 promoter, the administration route exerted a minimal effect on the transduction efficiency. These data provided a good reference for the selection of a suitable rAAV8 promoter for the gene therapy of liver diseases, as well as a suitable administration route. However, the molecular mechanism of differential efficiency between promoter CAG and TBG, as well as the dynamic comparison remain to be investigated.

Acknowledgements

Not applicable.

Funding

This study was supported by the Zhejiang Public Welfare Technology Research Program (grant no. LGD19H070001), the Zhejiang Provincial Natural Science Foundation of China (grant nos. LGF19H030008 and LY20H030001), the Ningbo Clinical Medicine Research Center Project (grant no. 2019A21003) and the Ningbo Public Welfare Technology Application Research Project (grant no. 202002N3160).

Availability of data and materials

The datasets used and/or analyzed during the current study are available from the corresponding author on reasonable request.

Authors' contributions

JK and LH performed the experiments, organized the figures and wrote the manuscript. WZ, JL and XZ collected and analyzed the data. YS and AL conceived the study, confirmed the authenticity of all the raw data and revised the manuscript. All authors have read and approved the final manuscript.

Ethics approval and consent to participate

The study was approved by the institutional animal care and use committee (approval no. IACUC 201903-138) at Ningbo University (Zhejiang, China).

Patient consent for publication

Not applicable.

Competing interests

The authors declare that they have no competing interests.

References

1. Ai J, Li J, Gessler DJ, Su Q, Wei Q, Li H and Gao G: Adeno-associated virus serotype rh.10 displays strong muscle tropism following intraperitoneal delivery. Sci Rep 7: 40336, 2017.
2. Wang D, Zhong L, Nahid MA and Gao G: The potential of adeno-associated viral vectors for gene delivery to muscle tissue. Expert Opin Drug Deliv 11: 345-364, 2014.
3. Dismuke DJ, Tenenbaum L and Samulski RJ: Biosafety of recombinant adeno-associated virus vectors. Curr Gene Ther 13: 434-452, 2013.
4. Lotfinia M, Abdollahpour-Alitappeh M, Hatami B, Zali MR and Karimipoor M: Adeno-associated virus as a gene therapy vector: Strategies to neutralize the neutralizing antibodies. Clin Exp Med 19: 289-298, 2019.
5. Vercauteren K, Hoffman BE, Zolotukhin I, Keeler GD, Xiao JW, Basner-Tschakarjan E, High KA, Ertl HC, Rice CM, Srivastava A, *et al*: Superior in vivo transduction of human hepatocytes using engineered AAV3 capsid. Mol Ther 24: 1042-1049, 2016.
6. Wang L, Bell P, Somanathan S, Wang Q, He Z, Yu H, McMenamin D, Goode T, Calcedo R and Wilson JM: Comparative study of liver gene transfer with AAV vectors based on natural and engineered AAV capsids. Mol Ther 23: 1877-1887, 2015.
7. Naso MF, Tomkowicz B, Perry WL and Strohl WR: Adeno-Associated Virus (AAV) as a vector for gene therapy. BioDrugs 31: 317-334, 2017.
8. Bates R, Huang W and Cao L: Adipose tissue: An emerging target for adeno-associated viral vectors. Mol Ther Methods Clin Dev 19: 236-249, 2020.
9. Mushimiyimana I, Niskanen H, Beter M, Laakkonen JP, Kaikkonen MU, Ylä-Herttuala S and Laham-Karam N: Characterization of a functional endothelial super-enhancer that regulates ADAMTS18 and angiogenesis. Nucleic Acids Res 49: 8078-8096, 2021.
10. Pham PL, Kamen A and Durocher Y: Large-scale transfection of mammalian cells for the fast production of recombinant protein. Mol Biotechnol 34: 225-237, 2006.
11. Powell SK, Rivera-Soto R and Gray SJ: Viral expression cassette elements to enhance transgene target specificity and expression in gene therapy. Discov Med 19: 49-57, 2015.
12. Lee LR, Peacock L, Lisowski L, Little DG, Munns CF and Schindeler A: Targeting Adeno-Associated Virus vectors for local delivery to fractures and systemic delivery to the skeleton. Mol Ther Methods Clin Dev 15: 101-111, 2019.
13. Daly TM, Okuyama T, Vogler C, Haskins ME, Muzyczka N and Sands MS: Neonatal intramuscular injection with recombinant adeno-associated virus results in prolonged beta-glucuronidase expression in situ and correction of liver pathology in mucopolysaccharidosis type VII mice. Hum Gene Ther 10: 85-94, 1999.
14. Kosuga M, Enosawa S, Li XK, Suzuki S, Matsuo N, Yamada M, Roy-Chowdhury J, Koiwai O and Okuyama T: Strong, long-term transgene expression in rat liver using chicken beta-actin promoter associated with cytomegalovirus immediate-early enhancer (CAG promoter). Cell Transplant 9: 675-680, 2000.
15. Chen SJ, Sanmiguel J, Lock M, McMenamin D, Draper C, Limberis MP, Kassim SH, Somanathan S, Bell P, Johnston JC, *et al*: Biodistribution of AAV8 vectors expressing human low-density lipoprotein receptor in a mouse model of homozygous familial hypercholesterolemia. Hum Gene Ther Clin Dev 24: 154-160, 2013.
16. Yan Z, Yan H and Ou H: Human thyroxine binding globulin (TBG) promoter directs efficient and sustaining transgene expression in liver-specific pattern. Gene 506: 289-294, 2012.
17. Wang Z, Zhu T, Rehman KK, Bertera S, Zhang J, Chen C, Papworth G, Watkins S, Trucco M, Robbins PD and Xiao X: Widespread and stable pancreatic gene transfer by adeno-associated virus vectors via different routes. Diabetes 55: 875-884, 2006.
18. Sobrevals L, Enguita M, Rodriguez C, Gonzalez-Rojas J, Alzaguren P, Razquin N, Prieto J and Fortes P: AAV vectors transduce hepatocytes in vivo as efficiently in cirrhotic as in healthy rat livers. Gene Ther 19: 411-417, 2012.
19. Cunningham SC, Dane AP, Spinoulas A and Alexander IE: Gene delivery to the juvenile mouse liver using AAV2/8 vectors. Mol Ther 16: 1081-1088, 2008.
20. Xu G, Dai M, Zheng X, Lin H, Liu A and Yang J: Cholestatic models induced by lithocholic acid and α-naphthylisothiocyanate: Different etiological mechanisms for liver injury but shared JNK/STAT3 signaling. Mol Med Rep 22: 1583-1593, 2020.
21. Livak KJ and Schmittgen TD: Analysis of relative gene expression data using real-time quantitative PCR and the 2(-Delta Delta C(T)) method. Methods 25: 402-408, 2001.

22. Niwa H, Yamamura K and Miyazaki J: Efficient selection for high-expression transfectants with a novel eukaryotic vector. Gene 108: 193-199, 1991.
23. Buck TM and Wijnholds J: Recombinant Adeno-Associated Viral Vectors (rAAV)-vector elements in ocular gene therapy clinical trials and transgene expression and bioactivity assays. Int J Mol Sci 21: 4197, 2020.
24. Acland GM, Aguirre GD, Bennett J, Aleman TS, Cideciyan AV, Bennicelli J, Dejneka NS, Pearce-Kelling SE, Maguire AM, Palczewski K, *et al*: Long-term restoration of rod and cone vision by single dose rAAV-mediated gene transfer to the retina in a canine model of childhood blindness. Mol Ther 12: 1072-1082, 2005.
25. Gardiner KL, Cideciyan AV, Swider M, Dufour VL, Sumaroka A, Komáromy AM, Hauswirth WW, Iwabe S, Jacobson SG, Beltran WA and Aguirre GD: Long-term structural outcomes of late-stage RPE65 gene therapy. Mol Ther 28: 266-278, 2020.
26. Carrillo-Carrasco N, Chandler RJ, Chandrasekaran S and Venditti CP: Liver-directed recombinant adeno-associated viral gene delivery rescues a lethal mouse model of methylmalonic acidemia and provides long-term phenotypic correction. Hum Gene Ther 21: 1147-1154, 2010.
27. Baruteau J, Waddington SN, Alexander IE and Gissen P: Gene therapy for monogenic liver diseases: Clinical successes, current challenges and future prospects. J Inherit Metab Dis 40: 497-517, 2017.
28. Erokhin M, Vassetzky Y, Georgiev P and Chetverina D: Eukaryotic enhancers: Common features, regulation, and participation in diseases. Cell Mol Life Sci 72: 2361-2375, 2015.
29. Greig JA, Nordin JM, Bote E, Makaron L, Garnett ME, Kattenhorn LM, Bell P, Goode T and Wilson JM: Impact of intravenous infusion time on AAV8 vector pharmacokinetics, safety, and liver transduction in cynomolgus macaques. Mol Ther Methods Clin Dev 3: 16079, 2016.
30. Chen BD, He CH, Chen XC, Pan S, Liu F, Ma X, Li XM, Gai MT, Tao J, Ma YT, *et al*: Targeting transgene to the heart and liver with AAV9 by different promoters. Clin Exp Pharmacol Physiol 42: 1108-1117, 2015.
31. Dalwadi DA, Torrens L, Abril-Fornaguera J, Pinyol R, Willoughby C, Posey J, Llovet JM, Lanciault C, Russell DW, Grompe M and Naugler WE: Liver injury increases the incidence of HCC following AAV gene therapy in mice. Mol Ther 29: 680-690, 2021.
32. Yu DL, Chow N and Wootton SK: JSRV intragenic enhancer element increases expression from a heterologous promoter and promotes high level AAV-mediated transgene expression in the lung and liver of mice. Viruses 12: 1266, 2020.
33. Li S, Ling C, Zhong L, Li M, Su Q, He R, Tang Q, Greiner DL, Shultz LD, Brehm MA, *et al*: Efficient and targeted transduction of nonhuman primate liver with systemically delivered optimized AAV3B vectors. Mol Ther 23: 1867-1876, 2015.
34. Greig JA, Calcedo R, Kuri-Cervantes L, Nordin JM, Albrecht J, Bote E, Goode T, Chroscinski EA, Bell P, Richman LK, *et al*: AAV8 gene therapy for crigler-najjar syndrome in macaques elicited transgene T Cell responses that are resident to the liver. Mol Ther Methods Clin Dev 11: 191-201, 2018.
35. Sabatino DE, Lange AM, Altynova ES, Sarkar R, Zhou S, Merricks EP, Franck HG, Nichols TC, Arruda VR and Kazazian HH: Efficacy and safety of long-term prophylaxis in severe hemophilia A dogs following liver gene therapy using AAV vectors. Mol Ther 19: 442-449, 2011.
36. Chandler RJ, LaFave MC, Varshney GK, Trivedi NS, Carrillo-Carrasco N, Senac JS, Wu W, Hoffmann V, Elkahloun AG, Burgess SM and Venditti CP: Vector design influences hepatic genotoxicity after adeno-associated virus gene therapy. J Clin Invest 125: 870-880, 2015.
37. Nault JC, Datta S, Imbeaud S, Franconi A, Mallet M, Couchy G, Letouzé E, Pilati C, Verret B, Blanc JF, *et al*: Recurrent AAV2-related insertional mutagenesis in human hepatocellular carcinomas. Nat Genet 47: 1187-1193, 2015.
38. Wang PR, Xu M, Toffanin S, Li Y, Llovet JM and Russell DW: Induction of hepatocellular carcinoma by in vivo gene targeting. Proc Natl Acad Sci USA 109: 11264-11269, 2012.
39. Smith JS, Tian J, Muller J and Byrnes AP: Unexpected pulmonary uptake of adenovirus vectors in animals with chronic liver disease. Gene Ther 11: 431-438, 2004.
40. Hinderer C, Katz N, Buza EL, Dyer C, Goode T, Bell P, Richman LK and Wilson JM: Severe toxicity in nonhuman primates and piglets following high-dose intravenous administration of an adeno-associated virus vector expressing human SMN. Hum Gene Ther 29: 285-298, 2018.
41. Mendell JR, Al-Zaidy S, Shell R, Arnold WD, Rodino-Klapac LR, Prior TW, Lowes L, Alfano L, Berry K, Church K, *et al*: Single-dose gene-replacement therapy for spinal muscular atrophy. N Engl J Med 377: 1713-1722, 2017.
42. Ginocchio VM, Ferla R, Auricchio A and Brunetti-Pierri N: Current status on clinical development of adeno-associated virus-mediated liver-directed gene therapy for inborn errors of metabolism. Hum Gene Ther 30: 1204-1210, 2019.
43. Grimm D and Büning H: Small but increasingly mighty: Latest advances in AAV vector research, design, and evolution. Hum Gene Ther 28: 1075-1086, 2017.
44. Kattenhorn LM, Tipper CH, Stoica L, Geraghty DS, Wright TL, Clark KR and Wadsworth SC: Adeno-associated virus gene therapy for liver disease. Hum Gene Ther 27: 947-961, 2016.